Diffusion and Reaction in Viscous-flow Tubular Reactor

F. A. CLELAND and R. H. WILHELM

Princeton University, Princeton, New Jersey

The effect on point and integral average conversion of chemical reaction, coupled with radial diffusion and radial distribution of reaction times in viscous-flow tubular reactors, is reported. Solutions are given for first-order reaction over an extensive range of dimensionless rate and time variables. An expression is given for a criterion of the conditions when the contribution of diffusion is so small that it may safely be disregarded as a variable. Another criterion also is given for the situation when diffusivity is so large, in comparison with other system constants, that the simple plug flow solution may be used without incurring more than a specified error.

The hydrolysis of acetic anhydride was studied in 1/4- and 1/2-in.-diam. reactors in 10- and 15-ft. lengths. Reynolds numbers were between 40 and 400 and temperatures between 25° and 35°C. It was found that the derived equations form a proper description of experiments in the smaller tube. Deviations from theory in the larger tube are explained in terms of free convection arising from nonisothermal conditions and from concentration gradients in the tube. Grashof criteria for initiation of convection in the system are discussed.

A liquid-phase first-order chemical reaction was studied under isothermal conditions in a tubular reactor in the laminar-flow region. In this region the concept of bulk contact time loses meaning; there is a distribution of contact times brought about by the parabolic velocity profile. This distribution causes a radial concentration gradient to be established which in turn tends to be diminished by molecular diffusion and under some conditions by free convection. Thus reaction, flow, and diffusional effects are related. The specific chemical reaction chosen for this study of interacting variables was the liquid-phase hydrolysis of acetic anhydride.

Few investigations of chemical reactions in laminar flow have been reported. Bosworth (*1*), conducting a theoretical investigation of the modification of the distribution of contact times by molecular diffusion in a tubular flow reactor, showed under what conditions the effects of diffusion may be neglected. Denbigh (*7*) derived an expression for conversion in a second-order reaction in laminar flow under conditions in which reactant and product diffusion may be neglected.

THEORY

A differential volume of fluid within a tubular flow reactor will be considered. In general, heat, mass, and momentum may be transferred to or from this elemental volume and a chemical component may undergo reaction within it. The present investigation is limited to an analysis of reactions occurring isothermally in laminar flow. Therefore only mass transfer equations will be used here.

Derivation of Differential Equation

Steady state, axial symmetry, and flow in the axial direction only are assumed. Mass balances for the n chemical components are as follows:

$$-v_z\left(\frac{\partial c_i}{\partial z}\right) + D_i\left(\frac{\partial^2 c_i}{\partial r^2} + \frac{1}{r}\frac{\partial c_i}{\partial r} + \frac{\partial^2 c_i}{\partial z^2}\right) - R_i = 0,\ i = 1, 2 \cdots n \quad (1)$$

v_z is the axial velocity; z is the axial coordinate measured from the reactor inlet; r is the radial coordinate measured from the tube axis; and c_i, D_i, and R_i are the concentration, molecular diffusivity, and reaction rate of the ith component, respectively. The terms represent the rate of accumulation due to flow, diffusion, and reaction, respectively.

If the velocity profile is described by Poiseuille's equation, axial diffusion is negligible compared with radial diffusion, and there is no volume change on reaction, then Equation (1) becomes

$$-v_0\left(1 - \left(\frac{r}{R}\right)^2\right)\frac{\partial c_i}{\partial z} + D_i\left(\frac{\partial^2 c_i}{\partial r^2} + \frac{1}{r}\frac{\partial c_i}{\partial r}\right) - R_i = 0,\ i = 1, 2 \cdots n \quad (2)$$

v_0 being the velocity of the central stream line, and R the tube radius.

If a certain chemical species is undergoing a first-order reaction, only the mass balance of this component need be considered, since R_i is independent of the concentration of other components. Equation (2) for an irreversible first-order reaction becomes

$$-v_0\left(1 - \left(\frac{r}{R}\right)^2\right)\frac{\partial c}{\partial z} + D\left(\frac{\partial^2 c}{\partial r^2} + \frac{1}{r}\frac{\partial c}{\partial r}\right) - kc = 0 \quad (3)$$

where k is the reaction-velocity constant. Equation (3) in dimensionless form is

$$-(1 - U^2)\frac{\partial C}{\partial \lambda} + \alpha\left(\frac{\partial^2 C}{\partial U^2} + \frac{1}{U}\frac{\partial C}{\partial U}\right) - C = 0 \quad (4)$$

F. A. Cleland is with Shell Development Company, Emeryville, California.

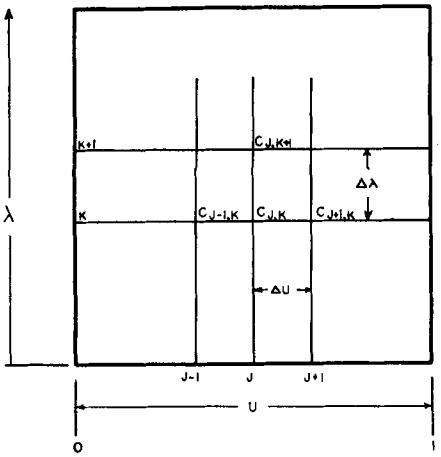

Fig. 1. Reference grid for difference-equation derivation.

where

$$\lambda = \frac{kz}{v_0}, \qquad C = \frac{c}{c_0}, \qquad \alpha = \frac{D}{kR^2},$$

and

$$U = \frac{r}{R}$$

c_0 is the concentration of reactant at $z = 0$. Boundary conditions for Equation (4) are taken as follows:

$$\lambda = 0 \qquad C = 1$$

$$U = 1 \qquad \frac{\partial C}{\partial U} = 0$$

Solution

No readily integrable analytical solution was obtained for Equation (4), however, it is possible to solve analytically for the maximum and minimum effects of the diffusion parameter α. As α becomes large without limit, the radial concentration gradients must necessarily vanish. The situation is now as though the reaction were occurring in "plug" flow. For this case the concentration of reactant leaving the reactor is given by

$$C = e^{-k\theta_{avg}} = e^{-k(z/v)_{avg}} = e^{-2\lambda} \quad (5)$$

With $\alpha = 0$, Equation (4) becomes

$$(1 - U^2)\frac{\partial C}{\partial \lambda} = -C \quad (6)$$

which has the solution

$$C = e^{-\lambda/(1-U^2)} \quad (7)$$

The average concentration by Equation (7) is then

$$C_a = 4\int_0^1 U(1 - U^2)e^{-\lambda/(1-U^2)}dU \quad (8)$$

Introducing the new variable $x = \lambda/(1 - U^2)$ and integrating by parts gives

$$C_a = e^{-\lambda}(1 - \lambda) + \lambda^2 \int_\lambda^\infty \frac{e^{-x}}{x}dx \quad (9)$$

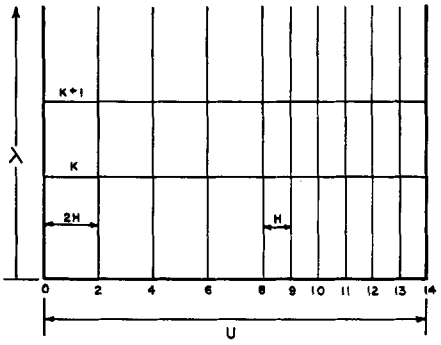

Fig. 2. Grid spacing for numerical integration.

The integral is the exponential integral, a tabulated function. For other values of α (including 0) Equation (4) was integrated numerically. As discussed later in this section, a comparison of the numerical and analytical solutions for $\alpha = 0$ affords a check of the numerical solution.

Method of Numerical Solution

Approximate solutions to differential equations may be obtained by numerical integration of corresponding difference equations.

Difference-equation formulation is by reference to the grid shown in Figure 1. Subscripts j and k refer to radial and axial positions, respectively. A Taylor's expansion of C about j, k is made in the axial and radial directions to evaluate the derivatives in Equation (4). Higher order terms in the Taylor's series are dropped, leading to an approximation in the derivatives. The radial Laplacian and the concentration term on the right in Equation (4) are averaged over the k and $k + 1$ rows to increase numerical stability (*13*) and thus speed up numerical computations. The resulting difference equation for the jth radial station is

$$\frac{(1 - U_j^2)(C_{j,k+1} - C_{j,k})}{\Delta\lambda} = \alpha\left[\frac{(C_{j+1,k+1} + C_{j-1,k+1} - 2C_{j,k+1} + C_{j+1,k} + C_{j-1,k} - 2C_{j,k}}{2(\Delta U)^2} + \frac{1}{4U_j\Delta U}(C_{j+1,k+1} - C_{j-1,k+1} + C_{j+1,k} - C_{j-1,k})\right] - \frac{C_{j,k+1} + C_{j,k}}{2} \quad (10)$$

This difference equation may be used for all points in the grid except

1. The tube wall, where the boundary condition, $\partial C/\partial U = 0$, must be applied
2. The tube center, where $(1/U)(\partial C/\partial U)$ is an indeterminate of the form 0/0. Applying L'Hospital's rule gives

$$\lim_{U\to 0}\frac{1}{U}\frac{\partial C}{\partial U} = \left(\frac{\partial^2 C}{\partial U^2}\right)_{U=0} \quad (11)$$

Using this expression for the radial Laplacian in Equation (4) and noting that $C_{j+1} = C_{j-1} = C_2$ at the tube axis yields the implicit difference equation

$$\frac{C_{o,k+1} - C_{o,k}}{\Delta\lambda} = \frac{2\alpha}{(\Delta U)^2}[C_{2,k+1} - C_{o,k+1} + C_{2,k} - C_{o,k}] - \frac{C_{o,k+1} + C_{o,k}}{2} \quad (12)$$

where C_o is the concentration at the tube axis. (*See* Figure 2.)

3. Any intermediate position where the radial grid-element size is changed.

Individual equations for these points together with Equation (10) constitute a set of simultaneous difference equations which correspond to Equation (4).

This system of simultaneous difference equations was solved for values of $\alpha = 0$, 0.01, 0.1, and 1.0 for the specified boundary conditions. Solution was by means of an electronic digital computer, the I.B.M. Card Programmed Calculator, wired to perform eight-digit floating-decimal arithmetic. Eleven radial stations were used in the grid. Grid spacing near the wall was one half that near the tube axis. (*See* Figure 2.) This spacing favors accurate evaluation of radial derivatives in the regions where they are large. Inspection of the system of difference equations shows that eleven simultaneous equations arise from a choice of eleven radial stations. These equations were solved by means of the Thomas method, a description of which is given by Bruce, Peaceman, Rachford, and Rice (*2*). Details of present work are given elsewhere (*5*).

Solution of these equations gives point values of C as a function of U and λ. An integral average concentration based on the volumetric flow rate also was obtained by the computer. For this computation the following integral was evaluated by Simpson's rule:

$$C_a = \frac{\int_0^R 2\pi rvC\,dr}{\int_0^R 2\pi rv\,dr} = 4\int_0^1 U(1 - U^2)C\,dU \quad (13)$$

In most cases computations were continued until the fraction unconverted, C_a, was depleted to about 0.02.

TABLE 1. THEORETICAL VALUES OF C_a AS A FUNCTION OF λ FOR VARIOUS VALUES OF α

$\lambda = kz/v_0$	$\alpha = 0$	$\alpha = 0.01$	$\alpha = 0.10$	$\alpha = 1.0$	$\alpha = \infty$
0	1	1	1	1	1
0.01	0.9810	0.9800	0.9806	0.9808	0.9802
0.02	0.9625	0.9608	0.9615	0.9615	0.9608
0.03	0.9447	0.9424	0.9428	0.9427	0.9418
0.04	0.9273	0.9246	0.9247	0.9242	0.9231
0.05	0.9105	0.9073	0.9071	0.9061	0.9048
0.07	0.8780	0.8743	0.8731	0.8710	0.8694
0.10	0.8328	0.8282	0.8251	0.8211	0.8187
0.15	0.7645	0.7585	0.7520	0.7443	0.7408
0.20	0.7037	0.6965	0.6863	0.6747	0.6703
0.25	0.6491	0.6409	0.6270	0.6116	0.6065
0.30	0.5999	0.5906	0.5733	0.5544	0.5488
0.35	0.5552	0.5452	0.5247	0.5026	0.4966
0.40	0.5145	0.5037	0.4803	0.4556	0.4493
0.45	0.4773	0.4661	0.4409	0.4130	0.4066
0.50	0.4432	0.4316	0.4033	0.3741	0.3679
0.60	0.3831	0.3711	0.3392	0.3076	0.3012
0.70	0.3321	0.3201	0.2856	0.2528	0.2466
0.80	0.2887	0.2768	0.2407	0.2079	0.2019
0.90	0.2514	0.2397	0.2030	0.1707	0.1653
1.00	0.2194	0.2082	0.1709	0.1403	0.1353
1.10	0.1918	0.1809	0.1446	0.1152	0.1108
1.20	0.1679	0.1576	0.1222	0.0946	0.0907
1.30	0.1472	0.1372	0.1031	0.0777	0.0743
1.40	0.1211	0.1199	0.0871	0.0638	0.0608
1.60	0.0998	0.0917	0.0621	0.0430	0.0408
1.80	0.0774	0.0702	0.0443	0.0290	0.0273
2.00	0.0603	0.0540	0.0316	0.0196	0.0183

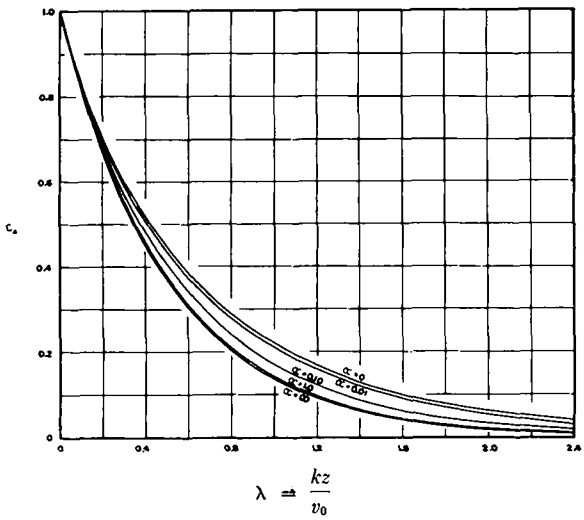

Fig. 3. Theoretical curves of C_a vs. λ with $\alpha = D/kR^2$, a parameter.

Solutions in Tables and Graphs

All point and integral average concentrations are available in printed I.B.M. tables. Range of variables is C_a from 1.0 to 0.02, λ from 0 to 2, α from 0 to 1.0. A brief table of selected values is provided in Table 1*.

Table 2 compares C_a for $\alpha = 0$ calculated from numerical integration (Table 1) and from analytical solution [Equation (9)]. Thus agreement between the two integrations is quite good.

*Complete data are available as document 5055 from the American Documentation Institute, Photoduplication Service, Library of Congress, Washington 25, D. C., at $5.00 for photoprints or $2.25 for 35-mm. microfilm.

TABLE 2.

COMPARISON OF C_a FROM NUMERICAL AND ANALYTICAL INTEGRATIONS FOR $\alpha = 0$

λ	C_a from analytical solution [Eq. (9)]	C_a from numerical integration
0.01	0.9806	0.9810
0.05	0.9098	0.9105
0.20	0.7039	0.7037
1.00	0.2194	0.2194
2.00	0.0603	0.0603

Figure 3 presents integral average concentrations as a function of α and λ. Typical concentration profiles for various values of λ with $\alpha = 0.1$ are given in Figure 4. The effect on concentration profiles of the diffusion parameter α at constant λ is illustrated in Figure 5.

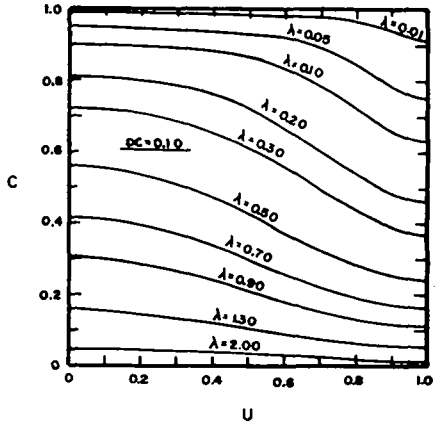

Fig. 4. Theoretical radial-concentration profiles at $\alpha = 0.1$.

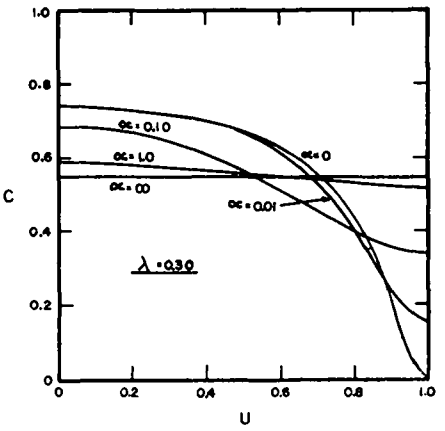

Fig. 5. Theoretical concentration profiles for various values of α with $\lambda = 0.3$.

Discussion of Theoretical Results

The solutions, Figure 3, show how the system parameters are bounded by conditions that represent the following physical situations: (1) radial diffusion is neglected but the parabolic flow profile is not ($\alpha = 0$) and (2) radial diffusion is very large or the tube diameter approaches zero ($\alpha = \infty$); this condition yields conversions equivalent to plug flow. C_a, the fraction unconverted, is highest when radial diffusion is negligible in extent and lowest when α approaches infinity. Curves for all values of the diffusion parameter converge at high and low values of λ. The convergence at low values of λ (as $C_a \rightarrow 1$) indicates that only small error is introduced in computing C_a through the assumption of parabolic flow directly at the tube entrance, when actually this condition is not approached until about $0.03 \times Re$ pipe diameters downstream (8).

Although this paper deals primarily with a first-order reaction, for comparison the two limiting curves for an irreversible second-order reaction ($2A \rightarrow B$) occurring in laminar flow are also presented, in Figure 6. Isothermal conditions and a constant-volume reaction are assumed. Both curves can be expressed analytically, the solutions being given by Denbigh (7).

TABLE 3. VALUES OF $D\theta_o/R^2$ REQUIRED TO LOWER C_a BY 1%

λ	C_a at $\alpha = 0$	α when $C_a = 0.99 \times (C_a$ at $\alpha = 0)$	$\alpha\lambda = D\theta_o/R^2 \times 10^3$
0.2	0.7037	0.00977	1.95
0.5	0.4432	0.00382	1.91
0.8	0.2887	0.00244	1.95
1.0	0.2194	0.00195	1.95
1.5	0.1135	0.00128	1.92
2.0	0.0603	0.000955	1.91

No diffusion ($\alpha = 0$):

$$C_a = 1 - 2\lambda'\left(1 - \lambda' \ln \frac{1+\lambda'}{\lambda'}\right) \quad (14)$$

Uniform radial concentration ($\alpha = \infty$):

$$C_a = \frac{1}{1 + 2\lambda'} \quad (15)$$

where $\lambda' = c_o k'\theta_o$ and $\alpha = D/k'c_o R^2$, k' being the rate constant for second-order reaction. Physical situations previously described as associated with the limiting curves for a first-order reaction also apply here. The modification in conversion brought about by a parabolic velocity profile and the relative magnitude of this effect between first- and second-order reactions may be illustrated by a numerical example.

Suppose an experimenter has studied a first-order chemical reaction in a batch system and that he wishes to perform the reaction also in a tubular reactor obtaining an 80% conversion in the latter. Referring to his batch reactor data, he finds the "contact time" required to obtain 80% conversion and translates this contact time to the flow reactor as follows:

$$\text{contact time} = \frac{\text{tube length}}{\text{average velocity}}$$

If he chooses flow rates such that flow is laminar and maintains isothermal conditions in the reactor, he will find that the conversion achieved in the tube is less than the desired 80% and, depending on conditions, might be as low as 71%. (Table 1). Were the reaction a second-order reaction with equal molal concentrations of reactants instead of a first-order reaction, and the investigator again wished to obtain 80% conversion in a tubular flow reactor, he would find upon translating the contact time as described above and maintaining laminar flow that fraction conversion again is less than the desired 80%, although never less than 76%.

Another interesting comparison concerns the magnitude of error which might be encountered in determining a rate constant from laminar-flow experiments. In the case where a first-order reaction is occurring and inlet and exit concentrations yield a value of C_a of 0.20, it is seen from Table 1 that λ lies somewhere between 0.805 and 1.070 depending on the value of α; thus, if the reaction were treated as occurring in plug flow ($\alpha = \infty$) when actually $\alpha = 0$, the rate constant determined would be in error by 25%.

Tabulated and plotted results of the computations for first-order reactions permit quantitative evaluation of the contributions of diffusion and flow profile on mean conversion for any desired set of circumstances. It is desirable, however, to provide statements of practical conditions when the contribution of diffusion may safely be neglected or when the contribution is so great that the simple plug-flow solution may be used, within known limit of error.

Criterion for Neglecting the Effect of Radial Diffusion. In a theoretical investigation Bosworth (*1*) considered radial diffusion as modifying the distribution of contact times in laminar flow. He concluded that radial diffusion may be neglected as a variable when

$$D\theta_o/R^2 < 3.1 \times 10^{-3} \quad (16)$$

θ_o being contact time of the central stream line. By considering the physical properties of gases and liquids, he showed that for liquid systems it is possible to have laminar flow and negligible diffusion; however, frequently in gaseous reactions the critical Reynolds number is exceeded and turbulent flow attained before conditions for neglecting radial diffusion are reached.

In the current work radial diffusion will be regarded as negligible when the fraction unconverted is less than 1% lower than it would be in the absence of diffusion. Interpolating at fixed λ gives α, which lowers C_a 1% from its value at $\alpha = 0$. The product of λ and α is found to be nearly constant at 0.00195 (Table 3). Thus radial diffusion may be neglected when

$$\alpha\lambda = \frac{D\theta_o}{R^2} = \frac{\pi}{2}\frac{Dz}{V} < 1.95 \times 10^{-3} \quad (17)$$

This criterion for neglecting radial diffusion agrees quite well with that of Bosworth, although the present approach is an alternate to his.

The third variant in Equation (16) expresses the criterion in terms of the volume flow rate V and reactor length z. If liquid-phase molecular diffusivities are assumed to be 10^{-5} sq. cm./sec.; gas-phase values, 0.1 sq. cm./sec.; and tube length 100 cm., then diffusion effects may be neglected when liquid-flow rates are larger than 1 cc./sec. and gas rates are greater than 10^4 cc./sec. The normal Reynolds criterion for the limit of the viscous-flow range shows that the above mentioned flow rate for liquids may be easily achieved within the viscous range for tube diameters that are reasonable for the assumed tube length. In the case of gases, however, the flow rates needed to make gaseous radial diffusion negligible (10^4 cc./sec.) are achieved only in tubes of 60-cm. radius or greater if the flow is to remain laminar. It is concluded, therefore, that radial diffusion may often be neglected as a significant variable in liquids but very rarely in gases.

Criterion for Condition that Plug-flow Limit Is Valid. Inspection of the computed $C_a - \lambda - \alpha$ results shows that conversions attained in plug flow are approached when $\alpha\lambda > 1$. Table 4 presents the size of errors encountered if plug-flow conversions ($\alpha = \infty$) are assumed when $\alpha\lambda$ actually is given a value of 1. Here it is seen that only at high conversions are appreciable errors introduced through this assumption. Flow rates needed to make $\alpha\lambda = (D\theta_o/R^2) > 1$ for a tube 100 cm. long are computed to be less than 10^{-3} cc./sec. for liquids and less than 10 cc./sec. for gases (diffusivities given previously being used).

TABLE 4. ERROR INVOLVED BY ASSUMING PLUG-FLOW CONVERSIONS WHEN $\alpha\lambda = 1$

λ	α	$C_{a-\infty}$	C_a	$C_{a-\infty}/C_a$
0.1	10	0.8187	0.8187	1.000
0.5	2	0.3679	0.3699	0.995
1.0	1	0.1353	0.1403	0.964
2.0	0.5	0.0183	0.0235	0.779

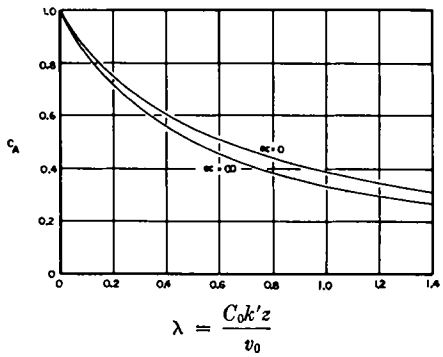

Fig. 6. Limiting curves of C_a vs. λ for a second-order reaction $2A \rightarrow B$.

EXPERIMENTAL

Chemical Reaction: Hydrolysis of Acetic Anhydride

This reaction satisfies requirements as a model reaction. It is pseudo first order,

has a half-life of a few minutes at moderate temperatures, and may be followed analytically with high accuracy. The kinetics of the reaction have been studied previously (*3, 9, 14, 16, 21*). Because of the need for constants to a higher temperature than was reported previously, kinetic experiments were undertaken.

The batch method was used. The vessel was a stirred glass flask; in a few runs stainless steel chips were added, with no measurable effect of the addition noted. Reaction temperatures were approximately 15°, 25°, and 35°C. Temperature was measured by means of a Beckmann thermometer, calibrated against a Bureau of Standards thermometer. Results are here reported for integer values of temperature, short interpolations to these values from the actual experimental conditions having been performed with the aid of the Arrhenius equation. The initial concentration of acetic anhydride was approximately 0.15*N*. Concentration of acetic anhydride in water solution was measured by the aniline-water method (*3, 21*). In this technique a sample of solution is introduced into a tared flask containing about fifteen times the amount of saturated aniline-water needed to react completely with the acetic anhydride in the sample; the reaction proceeds very rapidly compared with acetic anhydride hydrolysis and forms acetanilide, a nontitratable compound. The flask is then reweighed and the solution titrated with caustic soda by use of a phenothalein indicator.

These measurements together with a determination of the acetic acid present in a completely hydrolyzed sample permit calculation of the acetic anhydride concentration. Other details of the experiments are given elsewhere (*5*).

The validity of using a first-order expression for this reaction, when dilute, was verified. Four runs were made at 35°C., four at 25°C., and two at 15°C.

Average values of the measured experimental rate constants together with their 95% confidence limits are given in Table 5.

TABLE 5

T°C.	k, min.$^{-1}$	95% Confidence limits for k, %*
15.00	0.0817	1.12
25.00	0.1553	1.64
35.00	0.2733	1.32

*By Student's T test.

A least squares fit of the Arrhenius equation gave an energy of activation of 10.61 k.cal./g.-mole, the following being an expression of the temperature dependence:

$$\ln k = 16.0502 - \frac{5344.5}{T} \quad (18)$$

Temperature T is in degrees Kelvin.

Table 6 compares present rate constants with those previously reported.

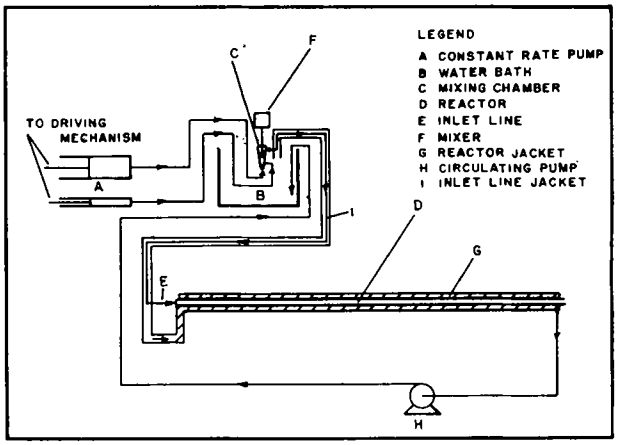

Fig. 7. Schematic diagram of apparatus.

TABLE 6. COMPARISON OF RATE CONSTANTS

T°C.	Acid N	k, min.$^{-1}$	Reference
25	0.15	0.1553 ± 0.0026	Present
	0.04	0.162	*14*
	0.23	0.156	
	0.07	0.1600	*21*
	0.015	0.1557	*3*
	0.15	0.1554	
	0.03–0.17	0.1587 (ave.)	*16*
15	0.15	0.0817 ± 0.0009	Present
	0.22	0.0806 ± 0.0002	*9*

Present value of k at 25°C. agrees with the values of all other investigators except Vles, who reported a value about 1.3% higher than the upper range of k (0.1579) here determined. The rate constant at 15°C. agrees well with that reported by Eldridge and Piret.

Viscous-flow Tubular Reactor

Conditions imposed in deriving Equation (4) were parabolic flow and constant temperature at all points in the reactor and uniform radial reactant concentration at the reactor inlet. A flow-reactor apparatus designed to approximate these conditions as closely as possible is illustrated in Figure 7.

Flow of reactants was induced by a constant-rate pump (*A*) with individual reservoirs for water and acetic anhydride. Reactants were pumped through coils in a constant-temperature water bath (*B*) to the mixing chamber (*C*) for mixing and dissolution of reactants. The mixer effluent, partially reacted acetic anhydride solution, flowed to the horizontal, jacketed reactor (*D*) through the jacketed inlet line (*E*). Fraction conversion of acetic anhydride within the reactor proper was determined from measurements of the inlet and outlet integral-average concentrations.

Sampling consisted of catching one sample of the flowing stream in a tared flask containing aniline-water and another in an empty tared flask, and allowing this sample to hydrolyze completely. Analysis of the two samples as described earlier permits the acetic anhydride concentration to be calculated. Inlet samples were taken at both the beginning and end of a run and several exit samples were taken during the run. A run was rejected if the exit concentration failed to remain constant for at least one residence time or if the initial and final inlet concentrations failed to agree.

The pump was a large, two-piston syringe designed for constant flow. A liquid-tight seal between the piston and cylinder was maintained by an O ring fitted into a grove in the piston. The glass cylinders, made by Scientific Glass Apparatus Company, were of precision-bore tubing 20 in. long. Inside diameters of the water and acetic anhydride tubes were 4 and ½ in. respectively, with bore tolerances of 0.0004 in. The constant-speed motor was wired for reversal of rotation, so that cylinders might be filled and emptied mechanically.

The pistons were advanced by a screw mechanism driven through a reduction box and gear train. Sets of gears with common centers were used to vary flow rates between experiments. Water rates from 11 to 170 cc./min. and acetic anhydride rates from 0.007 to 2.7 cc./min. were available. Flow rates from each cylinder had maximum deviations of about ±0.4% from the average. Calibration was made through the weight of liquid delivered in a measured time interval.

A large constant-temperature bath, controlled to ±0.01°C., was used to bring the fluid streams to reaction temperature and also to act as a reservoir from which water was circulated through the reactor jacket. The mixing chamber, submerged in the bath, was a 30-cc. conical glass vessel with entrance ports for water and acetic anhydride and an outlet for the solution. Agitation for the chamber was provided by a double-impeller stirrer which entered through an air-tight packing gland at the top of the chamber.

Dimensions for the reactors were as follows:

I.D., in.	Nominal length, ft.	Actual length, in.	Wall thickness, in.
0.248	15	182.3	0.065
0.248	10	121.3	0.065
0.496	15	183.1	0.065
0.496	10	123.2	0.065

All reactors were made of type-316 stainless steel tubing. The length of the reactors was determined in part by the requirement that parabolic flow exist in a substantial part of

TABLE 7. EXPERIMENTAL RESULTS

Run No.	Reactor Dia., in.	Reactor Length, in.	Temp., °C.	k, min.$^{-1}$	v_0, cm/sec.	C_0, moles/liter	Re	λ	C_a Experimental	C_a Theoretical	C_a $\alpha = 0$	C_a $\alpha = \infty$	α Experimental	α Theoretical	D_e/D
1	0.248	182.3	26.62	0.1704	4.58	0.0541	167	0.287	0.592	0.594	0.613	0.558	0.045	0.036	1.3
1A	"	"	26.62	"	6.85	0.0628	250	0.192	0.697	0.700	0.713	0.681	0.063	"	1.8
1B	"	"	26.62	"	4.58	0.0546	167	0.287	0.587	0.594	0.613	0.558	0.090	"	2.5
1C	"	"	26.62	"	3.05	0.0424	111	0.431	0.468	0.465	0.491	0.422	0.028	"	0.8
2	"	"	25.03	0.1556	1.146	0.0310	40.3	1.046	0.201	0.172	0.207	0.121	0.005	"	0.14
2B	"	"	25.00	0.1553	1.146	0.0222	40.3	1.046	0.139	0.172	0.207	0.121	0.45	"	13
2D	"	"	24.93	0.1547	1.146	0.0249	40.3	1.042	0.191	0.172	0.208	0.122	0.014	"	0.4
3	"	"	24.97	0.1550	4.58	0.0571	161	0.261	0.623	0.620	0.638	0.593	0.024	"	0.7
9C	"	121.3	35.00	0.2733	4.59	0.0467	199	0.305	0.571	0.578	0.595	0.543	0.063	0.025	2.5
11A	"	"	35.00	"	3.07	0.0601	133	0.456	0.441	0.452	0.473	0.403	0.040	"	1.6
11B	"	"	35.00	"	3.07	0.0625	133	0.456	0.439	0.452	0.473	0.403	0.049	"	2.0
8E	0.496	123.2	25.00	0.1553	1.141	0.0338	80.2	0.710	0.282	0.316	0.328	0.242	0.096	0.069	11
5C	"	183.1	35.00	0.2733	4.59	0.0548	398	0.462	0.435	0.461	0.469	0.397	0.063	0.006	11
5F	"	"	35.00	"	4.59	0.0552	398	0.462	0.428	0.461	0.469	0.397	0.11	0.006	18

the reactor length. In the least favorable reactor at the highest flow rate used about 4% of the tube length at the entrance is required in principle (*8*) for parabolic flow to be closely approached.

Reactors were connected to the inlet line through size 12/5 stainless steel semiball joints drilled out to ¼ in. I.D. These joints were silver-soldered directly to the ¼-in. reactors. They were connected to the ½-in. reactors through stainless steel joints 1-½ in. long and uniformly tapered from ¼ to ½ in. I.D.

Temperature in the water bath was measured with a Beckmann thermometer calibrated against a Bureau of Standards thermometer. Temperatures at the reactor extremities were measured with a thermistor inserted into the center of the entrance or exit stream. Axial center-line temperature profiles were obtained for various inlet reactant concentrations in a series of runs in which flow rates and inlet concentrations were varied systematically. The thermistor circuit used was a simple D.C. bridge circuit similar to the one described by Rand (*15*). Temperatures measured by this bridge were accurate to ±0.01°C.

Procedural details with respect to measurements, analysis, and constancy of conditions are available (*5*).

Treatment of Data

Measured variables were temperatures and inlet and exit concentrations, the flow rate being known from previous calibration. Values of the dimensionless groups C_a and λ were computed from these data and the reactor dimensions. The rate constant k was obtained from the batch-reactor data by use of the constant corresponding to the flow-reaction temperature. This temperature was taken as the water-bath temperature, as measurements of axial temperature profiles in the reactor showed the bath temperature to be a good measurement of the "average" reactor temperature. The "average" k, assumed to hold over the entire reactor, was in the least favorable cases a maximum of 1% different from any point value in the reactor.

A comparison of a measured value of C_a with the theoretical value may be made if a value is assigned to the diffusion parameter α, which is computed from the reaction-rate constant, the diffusion coefficient, and the tube radius. The diffusion coefficient is the only variable not previously established. The Wilke semiempirical correlation (*22*) was used to estimate the diffusion coefficient of acetic anhydride in water, giving 0.93×10^{-5} sq. cm./sec. at 25°C. and 1.23×10^{-5} sq. cm./sec. at 35°C.

A theoretical value of C_a may be found for the calculated α and λ by use of a cross plot of the theoretical results (Table 1). It was found that over a range of α from 0.01 to 1.0 a straight line results from plotting log α vs. C_a at constant λ. For values of α less than 0.01 a linear interpolation was used between values of C_a obtaining at 0 and 0.01. A theoretical value of C_a was determined for each run by this procedure.

Another comparison of theory and experiment may be made by computing an effective diffusion coefficient. By means of cross plot described in the preceding paragraph, a value of α is determined for the measured C_a and the effective diffusivity (D_e) is calculated from this α. Effective diffusion coefficients were calculated for all runs by this procedure; however, the values so obtained are subject to large deviations owing to the large change in α resulting from a relatively small change in C_a.

Entrance Flow Patterns

Flow patterns prevailing at the inlet of the ½-in.-diam. reactor were obtained through visual observation of the corresponding patterns in a ½-in. glass tube with a similar entrance. Dye was injected into the main stream as it passed through the ¼-in. inlet line. The glass tube, uniformly tapered from ½ in. to 5 mm. I.D. over a 1-in. transition length, had a 12/5 semiball joint attached for connecting it to the entrance line.

At low flow rates ($Re = 100$) a slight wavering was evident in a dye filament passing through the center of the entrance of the tube. This instability appeared to be damped out about 4 in. downstream from the entrance. In order to observe the entire flow pattern, the inlet line was flooded with dye with the water flow shut off; when flow was started, the entering stream appeared to "mushroom" after leaving the 5-mm. I.D. region. Outer filaments dispersed toward the tube wall, where they reversed direction and flowed back toward the inlet, rejoining the main stream at this point to form a circulating "doughnut" at the entrance. Central portions of the stream were in random motion for about 4 in. downstream from the entrance, where they were pulled into the parabola characteristic of laminar flow.

With higher flow rates ($Re = 400$) the dye patterns showed the entrance section to be turbulent for about 4 to 6 in. from the entrance, the flow appearing laminar beyond this distance. Turbulence in the entrance zone was sufficient to disperse a dye filament almost instantaneously over the entire cross section.

Flow patterns in the glass tube appeared the same whether the flowing stream was a reacting acetic anhydride solution or water alone.

RESULTS

The range of experimental variables is indicated in the following listing:

Temperature:	25° and 35°C.
Tube I.D.:	¼ and ½ in.
Tube length:	10 and 15 ft.
Linear velocity, v_0:	1.15 to 6.85 cm./sec.
Reynolds number:	40.3 to 398
$\lambda = kz/v_0$:	0.287 to 1.84
C_a, fraction unconverted:	0.04 to 0.71

Experimental data and computed dimensionless groups, C_a, λ, and α, as well as effective diffusion coefficients, D_e, and theoretical values of C_a, are presented in Table 7; for comparison, theoretical values of C_a at $\alpha = 0$ and $\alpha = \infty$ are also listed.

Axial center-line temperature profiles, measured to determine the approach to isothermal conditions, are presented for the ¼-in. reactor at 35°C. and for the ½-in. reactor at 25° and 35°C. in Figures 8, 9, and 10, respectively. Over-all radial

TABLE 7. EXPERIMENTAL RESULTS—(Continued)

Run No.	Reactor Dia., in.	Reactor Length, in.	Temp., °C.	k, min.$^{-1}$	v_o, cm/sec.	c_o, moles liter	Re	λ	C_a, Experimental	C_a Theoretical	C_a $\alpha = 0$	C_a $\alpha = \infty$	α Experimental	α Theoretical	$\frac{D_e}{D}$
3F	0.248	182.3	24.97	0.1551	4.58	0.0340	161	0.261	0.629	0.620	0.638	0.593	0.010	0.036	0.3
3G	"	"	25.00	0.1553	4.58	0.0579	161	0.261	0.622	0.620	0.638	0.593	0.028	"	0.8
4A	"	"	"	"	1.146	0.0299	40.3	1.046	0.160	0.172	0.207	0.121	0.113	"	3.1
4B	"	"	"	"	1.146	0.0300	40.3	1.046	0.179	0.172	0.207	0.121	0.015	"	0.4
9A	"	121.3	35.00	0.2733	4.59	0.0481	199	0.305	0.571	0.578	0.595	0.543	0.063	0.025	2.5
9B	"	"	"	"	4.59	0.0466	199	0.305	0.578	0.578	0.595	0.543	0.025	"	1.0
10B	"	"	"	"	1.149	0.0187	49.8	1.221	0.147	0.132	0.163	0.0870	0.050	"	2.0
10C	"	"	"	"	1.149	0.0197	49.8	1.221	0.155	0.132	0.163	0.0870	0.010	"	0.4
7A	0.496	123.2	25.00	0.1553	4.58	0.0554	322	0.1767	0.712	0.726	0.732	0.703	0.20	0.009	22
7B	"	"	"	"	4.58	0.0595	322	0.1767	0.714	0.726	0.732	0.703	0.14	"	16
8A	"	"	"	"	1.148	0.0880	80.8	0.705	0.285	0.319	0.330	0.244	0.10	"	11
8B	"	"	"	"	1.144	0.0585	80.5	0.708	0.289	0.317	0.329	0.243	0.068	"	7.6
5D	"	183.1	35.00	0.2733	4.59	0.0554	398	0.462	0.422	0.461	0.469	0.397	0.20	0.006	33
5E	"	"	"	"	4.59	0.0551	398	0.462	0.423	0.461	0.469	0.397	0.18	"	30
6A	"	"	"	"	1.147	0.0472	99.4	1.845	0.043	0.0686	0.0733	0.0249	0.11	"	18
6B	"	"	"	"	1.147	0.0472	99.4	1.839	0.042	0.0688	0.0739	0.0252	0.14	"	23

temperature gradients (center-line temperature T_0 minus wall temperature T_w) are plotted against average time of contact, inlet concentration being a parameter.

DISCUSSION

In this section it is shown that the derived equations for reaction, flow, and diffusion form a proper description of experimental results. However, it was found also that under certain circumstances free convection, which was not included through terms in the original rate equation, may be important in laminar-flow tubular reactors.

Theory is compared with experiment in Figure 8 through a plot of the corresponding values of C_a. Data obtained with the ¼-in. reactor are seen to fall quite well on a line of unit slope, an indication that for this reactor the variables are related as predicted by theory. The data scatter somewhat more at low values of C_a than at high values owing to lower precision of the analytical technique when small concentrations are measured. Data for the ½-in. reactor, however, fall consistently above the line, an indication of an experimentally significant difference between the ½- and ¼-in. reactors, the effect of this difference being to increase fraction conversion.

The higher conversion obtained in the ½-in. reactors may be explained if any one or combination of the following mechanisms are important in the ½-in. reactors and less so in the ¼-in. reactors:

1. Entrance effect causing radial mixing for an appreciable part of the reactor length.
2. Heat generation within the reactor and heat losses from the reactor causing conditions to be nonisothermal.
3. Natural convection within the reactor causing radial mixing to be much greater than would occur by molecular diffusion alone.

Of these the third effect appears to be the most important.

Entrance Effect. The maximum length of the ½-in. reactor in which there is disturbed flow prior to achievement of parabolic flow was 6 in. Computations (*5*) which assume uniform radial concentration in this early section and normal characteristics for the remainder of the tube show that at most only 10% of the discrepancy between C_a values of the two tube sizes (Figure 8) may be accounted for by entrance effects.

Thermal Effect. Maximum radial temperature gradients for an inlet acetic anhydride concentration of 0.06 mole/liter are shown in Figures 9, 10, and 11 to be as follows: 0.10°C. at 25°C., and 0.15°C. at 35°C. for the ½-in. reactor and about 0.05°C. at 35°C. for the ¼-in. reactor. A direct effect of this temperature rise is to increase the reaction-rate constant which in turn, through the dimensionless groups λ and α, affects the value of C_a. If it is assumed that the maximum temperature increase is effective throughout the tube, then a conservative estimate of the change in the rate constant k by use of the reactant temperature instead of the wall (or bath) temperature, is as follows: ½-in. reactor at 25°C., k increases by 0.6%, at 35°C. by 0.8%; ¼-in. reactor at 35°C., k increases by 0.3%. The maximum error introduced in the theoretical C_a through this direct effect of temperature rise in the tube is computed (*5*) to be no more than 15% of the difference between theoretical and experimental values of the C_a variable in the ½-in. reactor. The effect under discussion is negligibly small in the ¼-in. reactor.

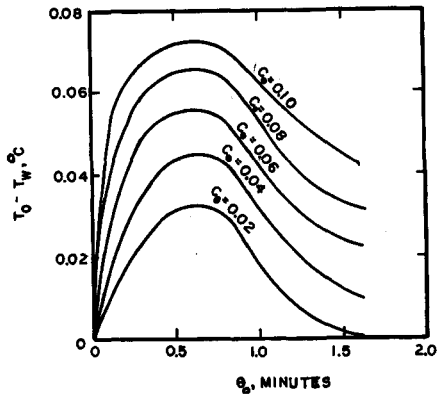

Fig. 8. Axial center-line temperature profiles for ½-in. reactor at 35°C.

Free Convection. Convective currents in a fluid may be established through a density gradient in the system or may be induced by mechanical vibration (*10*). The latter mode was minimized in this work through rubber connections and mountings for the pump. Only convection by density gradient is here considered important.

The convective process known as free convection or natural convection becomes established when the density gradient exceeds some critical value. The density gradient may be due to a temperature gradient, a concentration gradient, or a combination of the two. The convective processes cause mass and heat transfer rates within a fluid layer to be increased, so that, in effect, conductivities and diffusivities are increased.

Free-convection effects in nonflow systems usually are characterized by the following relationships:

heat transfer:

$$hL/K = F(Gr, Pr) \qquad (19)$$

mass transfer:

$$k''L/D = F(Gr, Sc) \qquad (20)$$

Very often the functionalities expressed in the preceding equations have been found to be of the form $c \times (GrPr)^n$ and $c \times (GrSc)^n$ where c and n are constants. When conditions are such that free convection is not present, the entire functions are constants and describe pure molecular diffusion and conduction.

When heat transfer process in one system is similar to mass transfer in another, the constants c and n obtained

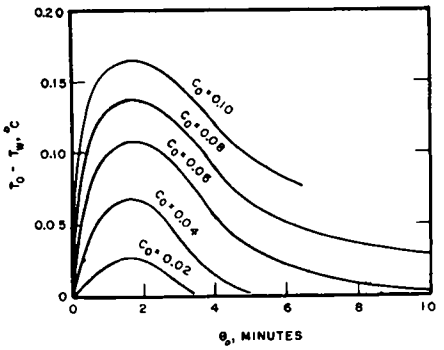

Fig. 9. Axial center-line temperature profiles for ½-in. reactor at 25°C.

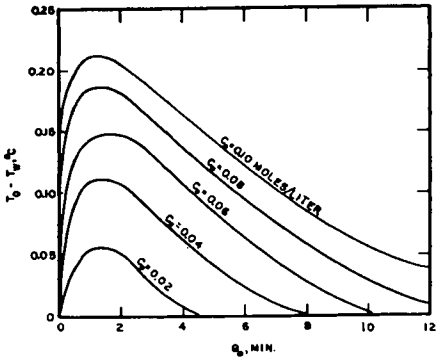

Fig. 10. Axial center-line temperature profiles for ½-in. reactor at 35°C.

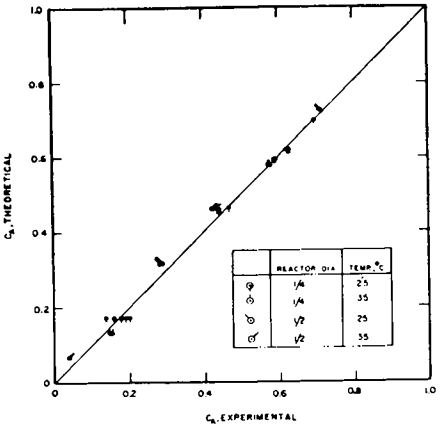

Fig. 11. Plot of experimental fraction unconverted against theoretical.

for one process may be used to describe the other. If free convection occurs in the presence of forced convection, the Reynolds number must also be included as a variable.

Studies of free convection fall into two classes: (1) initiation of free convection in a quiescent system, and (2) effects of free convection on heat and mass transfer rates. Experimental studies of the onset of free convection in a horizontal fluid layer heated from below are quite numerous (*4, 17, 18, 20*). These studies indicate that at a sharply defined value of the product of the Grashof and Prandtl numbers convection begins and that below this critical value no convection exists. Kraussold (*11*) reported data showing that the ratio of effective conductivity to molecular conductivity of a fluid is a universal function of *GrPr* for fluid layers confined in the annular space between horizontal concentric cylinders; at values of *GrPr* below a critical value, the ratio is unity and above this value increases with increasing values of *GrPr*.

Chandra (*4*) studied free convection in a horizontal air layer which was heated from below and subjected to a shear at the top surface. He found that the critical value of *GrPr* at which convection was established remained the same whether the layer was sheared or not. The initiation of free convection in a fluid flowing in a horizontal tube has not been studied, although studies have been made in flow systems to determine the effect of free convection on heat transfer (*6, 20, 12, 19*). These publications reveal that free convection may play a very important part in increasing heat transfer rates and that the effect of free convection is a function of the Reynolds number.

Since Chandra's work has shown that shear has no effect on the critical-density gradient at which convection begins in horizontal layers, it may perhaps be expected, by analogy, that the same criterion will hold for a fluid flowing in a tube as in the present investigation, i.e., that flow should remain laminar until some critical-density gradient is exceeded and that convection would be present for all gradients beyond the critical.

In the present work, if conditions are such that a critical value of the Grashof number (considering the Schmidt number constant) is exceeded in the ½- but not in the ¼-in. reactor, an increased effective diffusion coefficent and consequently an increased fraction conversion would be expected in the ½-in. reactor. Since the cube of the characteristic length term appears in the Grashof number, with all other variables constant, the Grashof number for the ½-in. reactor will always be eight times as large as for the ¼-in. reactor. Thus it is possible that the critical Grashof number lies between appropriate values of this group for the conditions obtaining within the ½- and ¼-in. reactors. Critical values of Grashof numbers for the reactors may be compared with critical values obtained in other systems. However, numerical values may be assigned to the Grashof numbers corresponding to the experimental runs only if the density gradients within the reactors are known.

Two factors may cause a radial density gradient within the reactors:

1. Concentration gradient due to greater depletion of reactant near the wall compared with that at the center of the reactor
2. Radial temperature gradients caused by heat released during reaction.

Direct knowledge of the density of acetic anhydride solutions is lacking because this system is a reacting one. With linear dilution properties assumed, extrapolation from the densities of pure acetic acid and anhydride to the reacting solution concentration leads to an estimate of 10^{-4} g./ml. for the maximum radial density gradient.

For the maximum temperature rise recorded in reaction experiments, i.e., 0.15°C. for the ½-in. reactor, the largest density gradient due to temperature rise was about 0.3×10^{-4} g./ml. Thus temperature and concentration appear to cause density gradients of the same order of magnitude.

Employing 10^{-4} g./ml. as a radial density gradient and the tube diameter as the characteristic length, one can compute Grashof group values as follows: ½-in. reactor at 35°C., 3,700; ½-in. reactor at 25°C., 2,400; ¼-in. reactor at 35°C., 460; ¼-in. reactor at 25°C., 300.

The measurements of Kraussold (*11*) showed that convection is not initiated until $GrPr > 1{,}000$ for horizontal annular liquid layers. If his results are extrapolated to zero inner cylinder diameter, the critical Grashof group, based on outer tube diameter, is 1,280 (*Pr* for water is taken as 6). This extrapolated value, which is derived for a physical arrangement similar to that in the present work, is noted to be between the Grashof group values for ½- and ¼-in. reactors. Support is thereby provided for the hypothesis that convection currents can be significant in viscous-flow tubular reactors.

An alternate manner of expressing the results of the reaction experiments is through the ratio of the effective to molecular diffusivity (*De/D*). The effective diffusivity is computed from experimental results applied to the present theory of viscous-flow reactors. Average values of this ratio for the two reactor sizes at both temperature levels are presented in Table 8.

Table 8. Average Diffusivity Ratios and Grashof Numbers for Experiment

Reactor diam., in.	Temperature, °C.	Diffusivity ratio *De/D*	Grashof No.
¼	25	1.1	300
¼	35	1.7	460
½	25	13.5	2,400
½	35	22.2	3,700

The value of the diffusivity ratio is noted to be close to unity for low values of the Grashof number with a rapid rise in the value of the ratio at larger values of the group. This characteristic relationship is similar to that presented by Kraussold for the ratio of effective to molecular conductivity for heat transfer to annular liquid layers.

Effective Diffusivities and Thermal Con-

ductivities. Insight may be obtained concerning the results of convective processes by a consideration of the degree to which the ratio of effective to molecular diffusivity will be different from the corresponding ratio for thermal conductivities within a given system.

In fluid layers the ratios hL/K and $k'L/D$ are, respectively, equivalent to Ke/K, the conductivity ratio, and De/D, the diffusivity ratio. For conditions of similarity for thermal conductive and diffusional processes by free convection, and from relations presented earlier in the paper, the following relation may be written:

$$\frac{De/D}{Ke/K} = \left(\frac{Sc}{Pr}\right)^n$$

A unique Grashof group for the system has been canceled from the earlier expressions in achieving the foregoing expression.

In gases Schmidt and Prandtl numbers have about the same value, and so De/D is approximately equal to Ke/K. In liquids, however, the Schmidt number is much higher than the Prandtl number. For example, the Schmidt number for many water solutions is about 1,000, and the Prandtl number is about 5. The ratio given above thus becomes

$$De/D = Ke/K(200)^n$$

The coefficient n has usually been found experimentally to be about ¼ to ⅛, and so the ratio of the groups De/D to Ke/K is about 5 or 6.

Because of the large value of $(De/D)/(Ke/K)$ in liquids it follows that in such systems convective effects will be detected more readily on measurement of mass diffusion than of thermal diffusion. From the view of detecting convective effects the experimental diffusion-reaction method such as the present study would thus seem to have advantages over a heat transfer approach to the subject.

ACKNOWLEDGMENT

Grateful acknowledgment is made to the Shell Development Company for a research grant in support of this study, to the E. I. duPont de Nemours Company for a postgraduate fellowship, and to the Humble Oil and Refining Company for making available an electronic computer on which some of the calculations were performed during one summer. The bulk of the calculations were made at the Forrestal Research Center, Princeton University, with the guidance of Dr. Forman S. Acton, which is hereby acknowledged.

The advice of Professor J. C. Whitwell of the Chemical Engineering Department, Princeton University, on statistical design of experiment and that of Dr. H. H. Rachford, of the Humble Oil and Refining Company, and of Dr. J. Beek, Jr., of the Shell Development Company, on other mathematical and computational aspects of the work were valuable and are also acknowledged with thanks. The authors wish to express appreciation to D. W. Peaceman, of the Humble Oil and Refining Company, for his careful review and valuable suggestions and in particular for pointing out the analytical integration of Equation (4) for $\alpha = 0$.

NOTATION

Units

L = length
M = mass
Q = quantity of heat
T = temperature
θ = time

---

c = point concentration of reactant, M/L^3
c_o = concentration of reactant at reactor inlet, M/L^3
C = point concentration of reactant = c/c_o, dimensionless
C_a = integral average concentration of reactant as defined in text, dimensionless
C_p = heat capacity of fluid, Q/MT
D = molecular diffusivity, L^2/θ
De = effective diffusivity as defined in text, L^2/θ
f = integral average fraction unconverted, $= 1 - C_a$, dimensionless
g = acceleration due to gravity, L/θ^2
G_r = Grashof number = $gL^3\rho^2\Delta\rho/\mu^2$, dimensionless
h = heat transfer coefficient, $Q/\theta L^2 T$
i = one of the n chemical components undergoing reaction
j = radial station in the grid used in numerical integration
k = reaction velocity constant, first order, θ^{-1}
k = axial station in grid used in numerical integration
k' = reaction-velocity constant, second order, $\theta^{-1}M^{-1}L^3$
k'' = mass transfer coefficient, mass per unit time, unit concentration difference, and unit cross-sectional area, $M/\theta ML^{-3}L^2$
K = thermal conductivity, $Q/\theta L^2 TL^{-1}$
Ke = effective thermal conductivity, $Q/\theta L^2 TL^{-1}$
L = characteristic length term, L
n = number of chemical components undergoing reaction
Pr = Prandtl number = $C_p\mu/K$, dimensionless
r = radial position in reactor measured from reactor axis, L
R = reactor radius, L
Re = Reynolds number = $2R\rho v_{avg}/\mu$, dimensionless
R_i = reaction rate of the jth chemical species, $M/L^3\theta$
Sc = Schmidt number $\mu/\rho D$, dimensionless
T = temperature of system, T
U = radial coordinate measured from reactor axis, $U = r/R$, dimensionless
v_o = velocity of central stream line within reactor, L/θ
v_{avg} = average velocity of fluid within reactor = $v_0/2$, L/θ
V = volumetric flow rate within reactor, L^3/θ
z = distance coordinate measured from reactor inlet, L
α = diffusion parameter = D/kR^2, dimensionless
η = kinematic viscosity = μ/ρ, L^2/θ
θ = time
θ_{avg} = average time of contact of fluid within reactor = reactor volume/volume flow rate, θ
θ_0 = time of contact of central stream line within reactor, θ
μ = viscosity of fluid, $M/L\theta$
ρ = density of fluid, M/L^3
λ = time of contact, $\lambda = kz/v_o$, dimensionless
λ' = time of contact, $\lambda' = c_o k' z/v_o$

LITERATURE CITED

1. Bosworth, R. C. L., *Phil. Mag.*, **39**, No. 7, 847 (1948).
2. Bruce, G. H., D. W. Peaceman, H. H. Rachford, Jr., and J. D. Rice, *Am. Inst. Mining Met. Engrs., Petroleum Trans.*, **198**, 79 (1953).
3. Caudri, J. F. M., *Rec. trav. chim.*, **49**, 1 (1930).
4. Chandra, K., *Proc. Roy. Soc. (London)*, **A164**, 231 (1938).
5. Cleland, F. A., Ph.D. dissertation, Princeton University, Princeton, N. J. (May, 1954).
6. Colburn, A. P., *Trans. Am. Inst. Chem. Engrs.*, **19**, 174 (1933).
7. Denbigh, K. G., *J. Applied Chem. (London)*, **1**, 227 (1951).
8. Eckert, E. R. G., "Introduction to the Transfer of Heat and Mass," 1 ed., McGraw-Hill Book Company, Inc., New York (1950).
9. Eldridge, J. W., and E. L. Piret, *Chem. Eng. Progr.*, **46**, 290 (1950).
10. Kern, D. Q., and D. F. Othmer, *Trans. Am. Inst. Chem. Engrs.*, **39**, 517 (1943).
11. Kraussold, H., *Forsch. Gebiete Ingenieurw.*, **5**, 186 (1934).
12. Martinelli, R. C., and L. M. K. Boelter, *Univ. Calif. Publ. Eng.*, **5**, 23 (1942).
13. O'Brien, G. G., M. A. Hyman and S. Kaplan, *J. Math. Phys.*, **29**, 223 (1951).
14. Orton, K. J. P., and M. Jones, *J. Chem. Soc. (London)*, **101**, 1708 (1912).
15. Rand, M. J., and L. P. Hammett, *J. Am. Chem. Soc.*, **72**, 287 (1950).
16. Rivett, A. C. D., and N. V. Sidgwick, *J. Chem. Soc. (London)*, **97**, 732 (1910).
17. Schmidt, R. J., and S. W. Milverton, *Proc. Roy. Soc. (London)*, **A152**, 586 (1935).
18. Schmidt, R. J., and O. A. Saunders, *Proc. Roy. Soc. (London)*, **A165**, 216 (1938).
19. Sieder, E. N., and G. E. Tate, *Ind. Eng. Chem.*, **28**, 1429 (1936).
20. Sutton, O. G., *Proc. Roy. Soc. (London)*, **A204**, 297 (1950).
21. Vles, S. E., *Rec. trav. chim.*, **52**, 809 (1933).
22. Wilke, C. R., *Chem. Eng. Progr.*, **45**, 218 (1949).